

Multiple recollisions in nonsequential double ionization below the recollision-ionization threshold

Xiao-Meng Ma(马晓萌), Ai-Hong Tong(童爱红), Zhuo Wang(王茁), and Chun-Yang Zhai(翟春洋)

Citation: Chin. Phys. B, 2021, 30 (**12**): 123402. DOI: 10.1088/1674-1056/ac2d1e
Journal homepage: http://cpb.iphy.ac.cn; http://iopscience.iop.org/cpb

What follows is a list of articles you may be interested in

Evidence of potential change in nonsequential double ionization

Changchun Jia(贾昌春), Pu Zhang(张朴), Hua Wen(文华), and Zhangjin Chen(陈长进)
Chin. Phys. B, 2021, 30 (**2**): 023401. DOI: 10.1088/1674-1056/abc151

Quantitative rescattering theory for nonsequential double ionization

Zhangjin Chen(陈长进), Fang Liu(刘芳), Hua Wen(文华)
Chin. Phys. B, 2019, 28 (**12**): 123401. DOI: 10.1088/1674-1056/ab54b3

A double toroidal analyzer for scanning probe electron energy spectrometer

Xu Chun-Kai, Zhang Pan-Ke, Li Meng, Chen Xiang-Jun
Chin. Phys. B, 2014, 23 (**7**): 073402. DOI: 10.1088/1674-1056/23/7/073402

Total cross sections for electron scattering from sulfur compounds

Tan Xiao-Ming, Wang Yan-Wen
Chin. Phys. B, 2013, 22 (**2**): 023403. DOI: 10.1088/1674-1056/22/2/023403

Total cross sections for electron scattering from fluoromethanes: A revised additivity rule method

Tan Xiao-Ming, Zhao Gang
Chin. Phys. B, 2012, 21 (**6**): 063402. DOI: 10.1088/1674-1056/21/6/063402

Multiple recollisions in nonsequential double ionization below the recollision-ionization threshold*

Xiao-Meng Ma(马晓萌)[1,2,†], Ai-Hong Tong(童爱红)[1,2], Zhuo Wang(王茁)[1,2], and Chun-Yang Zhai(翟春洋)[3]

[1] *Department of Physics and Mechanical & Electrical Engineering, Hubei University of Education, Wuhan* 430205, *China*
[2] *Institute of Optoelectronic Materials and Components, Hubei University of Education, Wuhan* 430205, *China*
[3] *College of Physics and Electronic Engineering, Xinyang Normal University, Xinyang* 464000, *China*

(Received 18 July 2021; revised manuscript received 22 September 2021; accepted manuscript online 6 October 2021)

By using the three-dimensional classical ensemble model, the recollision dynamics in nonsequential double ionization (NSDI) of Ar by 780-nm laser pulses at $(6–1.2)\times10^{14}$ W/cm^2 was extensively studied. We revealed the picture of multiple-recollision in the double ionization events at the laser intensity region below the recollision-ionization threshold. Via tracing the NSDI trajectories, it was found that the contribution of these multiple-recollision events increases as the laser intensity decreases. In this low intensity region, many multiple-recollision induced NSDI trajectories occur through the doubly excited states. The decay speed of the doubly excited state decreases with the decreasing laser intensity.

Keywords: nonsequential double ionization, multiple recollision

PACS: 34.80.–i, 79.70.+q, 45.50.Tn **DOI:** 10.1088/1674-1056/ac2d1e

1. Introduction

In the past two decades, nonsequential double ionization (NSDI) has been extensively investigated for its responsibility to significantly improve the double ionization yields.[1–6] The phenomenon is attractive because the double ionization yield is measured by many orders of magnitudes enhanced. Many works have been launched in order to study the underlying mechanism and now the widely accepted one as the primary picture is the recollision process: the first ionized electron leaves the nuclear and is driven back by the laser field, causing the direct ionization (RDI) or excitation (RESI) of the second electron through the energy exchange in the recollision.[7–12] It is this kind of interaction that results in the strong correlation between the two ionized electrons.[13] With the development of the ultrafast laser technology,[14–20] the study of NSDI becomes more extensive, and more fancy phenomenons in the correlated electron momentum spectra and sum-energy spectra were found.[21–25] For example, in the experiment on NSDI of helium by laser pulses at relatively low laser intensities, V-like (finger-like) structure in the correlated momentum distribution was observed.[26] Theoretical studies have shown that both the nuclear attraction and the final-state electron–electron repulsion play important roles.[27] But at high laser intensities, it has been shown that for the V-like structure, the asymmetric energy sharing between the two electrons at recollision is the decisive reason.[28,29] At lower laser intensities, it has been represented that NSDI occurs through doubly excited states and the decay dynamics of the doubly excited states has been detailedly explored by Camus *et al*.[30]

In the early stage, though it is known that the tunneled electron driven by the oscillating electric field of the linearly polarized laser pulse can return many times to the parent ion, people always regarded only once effective recollision that occurs at the first or the last return or the closest approach. In fact, the recollision picture is more complicate. For example, recent experiments on above threshold ionization have showed that the multiple-recollision event contributes to the low-energy peaks in the photoelectron energy spectrum.[31–34] In NSDI, multiple-recollision have also been already well speculated. For instance, Liu and Ye *et al*. have discussed that multiple-recollision may be responsible for the observed back-to-back emission of the correlated electron pairs for NSDI at low laser intensity.[35,36] They explained the long high-energy tail of the sum-energy spectrum is the consequence of increased number of multiple-recollision trajectories and found the percentage of multiple-recollision trajectories contributing to DI exhibits a significant increasing when the laser intensity reduces from 0.6×10^{14} W/cm^2 to 0.3×10^{14} W/cm^2. In a very recent experiment on NSDI by mid-infrared laser pulse, several small peak structures in the electron momentum spectrum were observed.[37] Associated with the multiple-recollision induced low-energy structures in strong-field above threshold ionization,[33] they are believed to be the symbolization of multiple recollisions in NSDI. But up to now, no clear-cut theoretical study has been performed to demonstrate the multiple recollisions in NSDI.

In this paper, with the three-dimensional (3D) fully classical ensemble model, we discuss the recollision dynamics in

*Project supported by the Natural Science Foundation of Hubei Province, China (Grant No. 2020CFB362), Scientific Research Program of Hubei Provincial Department of Education, China (Grant No. B2020176), and the National Natural Science Foundation of China (Grant No. 12104389).

†Corresponding author. E-mail: maxiaomenghue@126.com

© 2021 Chinese Physical Society and IOP Publishing Ltd

NSDI by linearly polarized laser pulses. Via tracing the NSDI trajectories, we find that multiple recollisions have a significant contribution to the NSDI yields when the laser intensity is below the recollision ionization threshold. Because of the multiple energy-exchange from recollisions, the energies of the doubly excited states are higher than those induced by single-recollision trajectories, resulting in the faster DI. As the intensities increases, the time delay distributions of the single-recollision and multiple-recollision NSDI events tend to be similar. In addition, we investigate the time evolution of each trajectories in NSDI which shows the contribution of multiple recollisions.

2. Method

The 3D classical ensemble model has been introduced for decades[38–41] and widely used in investigating the physical mechanism of NSDI process.[21,22,29,41–49] In this paper, we employ the method proposed by Eberly *et al*. to study the underlying recollision processes of NSDI.[38]

In this classical model, the evolution of the three-particle system is determined by the Newton's equation of motion (atomic units are used throughout until stated otherwise)

$$\frac{\mathrm{d}^2\boldsymbol{r}_i}{\mathrm{d}t^2} = -\nabla[V_{\mathrm{ne}}(\boldsymbol{r}_i) + V_{\mathrm{ee}}(\boldsymbol{r}_1,\boldsymbol{r}_2)] - \boldsymbol{E}(t), \tag{1}$$

where the subscript $i = 1$ or 2 is the label of the two electrons, and $\boldsymbol{E}(t)$ is the electric field, which is linearly polarized along the $\hat{x}$ axis and has a trapezoidal pulse shape with two-cycle turn on, six cycles at full strength, and two-cycle turn off. The soft Coulomb potential $V_{\mathrm{ne}}(\boldsymbol{r}_i) = -2/\sqrt{\boldsymbol{r}_i^2 + a^2}$ represents the ion-electron interaction and $V_{\mathrm{ee}}(\boldsymbol{r}_1,\boldsymbol{r}_2) = 1/\sqrt{(\boldsymbol{r}_1 - \boldsymbol{r}_2)^2 + b^2}$ is the electron-electron interaction. The soft parameter $a = 1.5$ is introduced here to avoid the autoionization[39] and b is set to be 0.1 to allow strong electron correlation.

To obtain the initial conditions for Eq. (1), the ensemble is populated starting from a classically allowed position for the argon ground-state energy of -1.59 a.u. The available kinetic energy is distributed randomly between the two electrons in the momentum space. Then the system is allowed to evolve for a sufficient long time (100 a.u.) before the laser field is turned on to obtain stable position and momentum distributions.

In our calculations, the ensemble size we perform is 2×10^6. When the laser field is turned off, we check the energies of both electrons, and the DI event is determined if both electrons achieve positive energies. Here the collision events denote the trajectories which satisfy the condition when the distance between two electrons $r_{12} < 2.0$ a.u. We define the single ionization time as the time when the first electron's energy achieves positive or the electron is outside the nuclear well, and the energy exchange between the two electrons is not zero. Traveling time indicates the time period between the recollision and the ionization of the recollision electron.

3. Results and discussion

Figure 1(a) shows the NSDI yields that we calculated by 3D absolute classical method, which well reproduces the NSDI featured "knee" structure for argon by linear polarized, 780-nm laser pulses. Here we classify the NSDI trajectories according to the times of recollisions. For the trajectories in which returning electrons visit the area $r_{12} < 2.0$ a.u. once, we called them as the single-recollision trajectories and for twice, the double-recollision trajectories. In our calculations, up to five or more recollisions were observed. In addition to the trajectories of once-recollision and twice-recollision, the electron trajectories with three times of recollision contributed the largest. We did not study the trajectories that the electron undergo three or more times of recollisions because the proportion of these trajectories is too small (less than 5%). Figures 1(b) and 1(c) present the proportion of the single-recollision and double-recollision events in the NSDI yield as a function of laser intensity, respectively. In order to observe the transformation of NSDI yield more clearly, we then calculate the ratio of double-recollision events to single-recollision events and show it in Fig. 1(d). It is clearly shown that with the increasing of intensity, the contribution of single-recollision trajectories to NSDI rises drastically when the intensity is below the recollision-ionization threshold and then the change tends to be gentle when the intensity is greater than 0.4×10^{14} W/cm^2. Absolutely opposite to it, the contribution of double-recollision events falls fast and then stays in a near platform state with the intensity increasing. That is to say, at the relatively low intensity, the phenomenon of multiple-recollision will be more distinct. It is easy to understand, because when the laser intensity increases, the recollision energy of the electron raises and thus the recollsion electron just needs one recollision to excite or ionize directly the bound electron.

To intuitively attest the processes stated above, three sample NSDI trajectories selected of electrons are clearly displayed in Fig. 2. In this report, we concentrate on the intensities below the recollision-ionization threshold. We examine the time evolutions of the energies of the two electrons, and the distance between the two electrons and the longitudinal (in the direction parallel to the laser polarization) momentum of each electron, respectively. For the NSDI trajectory shown in the left column, the recollision electron undergo only once collision at the first return at about $2.37T$ (T is the laser period), which has been indicated by the cyan arrows. The struck electron thus obtains a quantity of energy from the recollision electron and stays in the excited state for a period of time and then gets ionized by the field, i.e., the RESI is prevalent. In Fig. 2(d), after the first ionization of the recollision electron at

about $2.8T$, the distance between the two electrons suddenly reduce to $r_{12} < 2.0$ a.u. only once. Similarly, the longitudinal momenta of the recollision electron suffers once large sudden decrease after the recollision [in Fig. 2(g)]. For the NSDI trajectory shown in the middle column, just before the zero crossing of the laser electric field at about $2.42T$, the recollision electron experience the first impact with the struck electron. But the energy transferred is not enough to ionize the struck electron directly, so after the recollision the struck electron stays in an excited state for a period of time. It can be seen that the recollision electron then leave the nuclear and return after about half optical cycle. The struck electron gets ionized by the second recollision merely after the next electric field peak at about $2.84T$. This means that the first recollision occurs at the first returning of the recollision electron and the second collision occurs at the second returning. The energy exchange once again makes the bound electron hold enough energy to be ionized, so the time interval between the emission of the bound electron and the last recollision is very short. The NSDI trajectory shown in the right column also undergoes two recollisions, but the second recollisin occurs at the fourth returning after about $1.6T$ than the first recollision. For the two impacts we can see the obviously dramatically changes in the time evolution of the energy, the distance and the longitudinal momenta, which have also been pointed out by the cyan arrows.

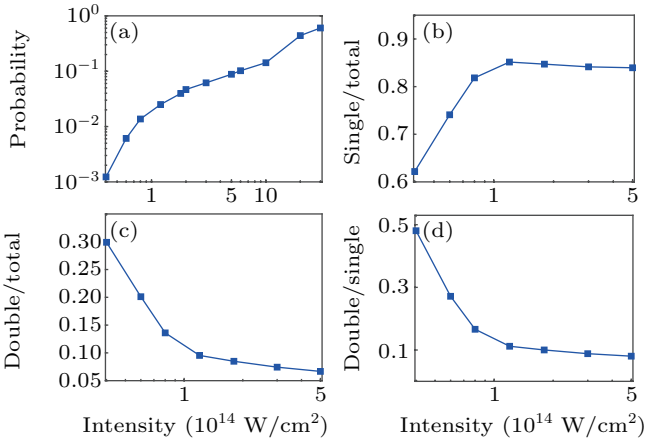


Fig. 1. (a) The "knee" structure NSDI yields for linear polarized, 780-nm laser pulses with different intensity. (b) Proportion of the single-recollision events in the total NSDI yield as a function of laser intensity at the wavelength of 780 nm. (c) Proportion of the double-recollision events in the total NSDI yield as a function of intensity at the wavelength of 780 nm. (d) Ratio of double-recollision events to single-recollision events from (b) and (c).

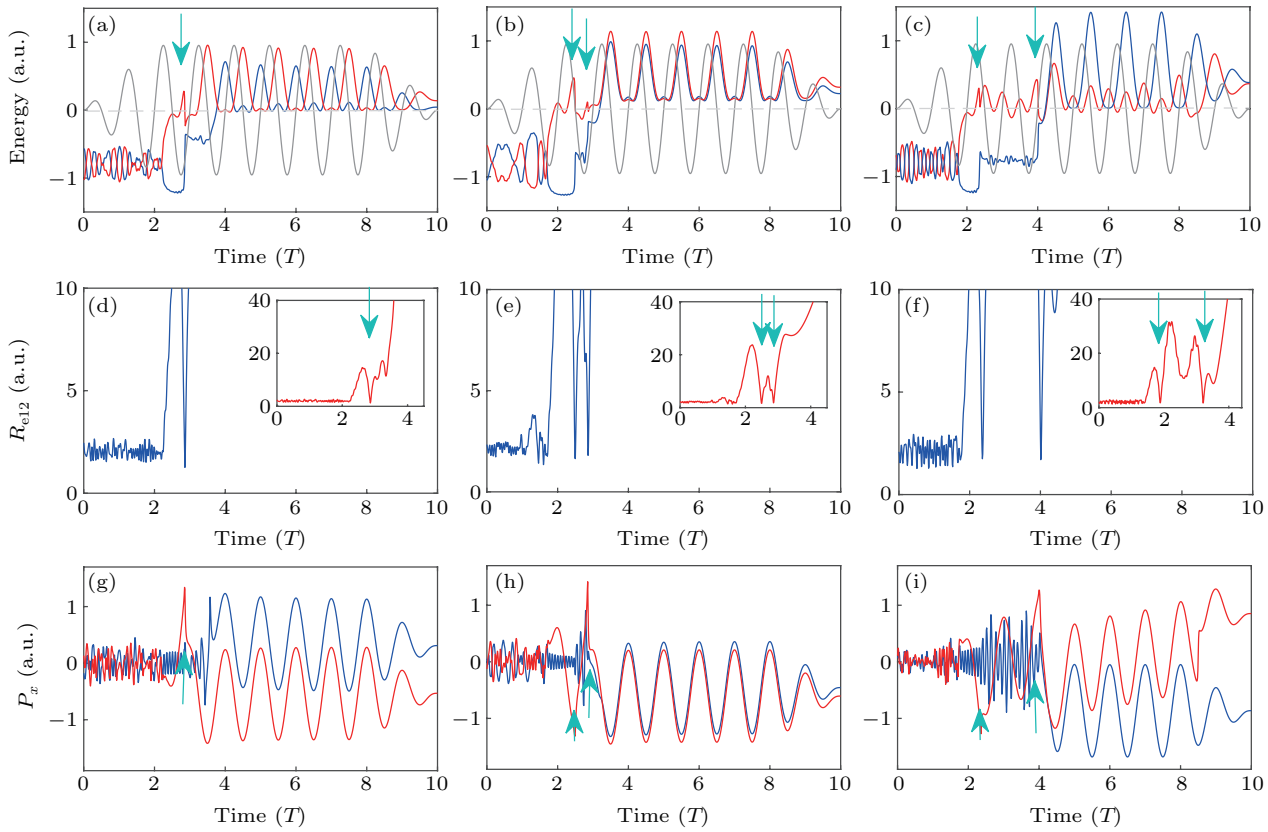


Fig. 2. Three illustrative NSDI trajectories selected from single-recollision events and double-recollision events at the intensity of 0.8×10^{14} W/cm^2. There is only one recollision in (a), (d), (g); and two recollisions in (b), (e), (h), (c), (f), (i). The panels from top to bottom show the energies of the two electrons, distance between the two electrons and the longitudinal momenta of each electron versus the time, respectively. The inserted maps in the second row indicate the corresponding amplification. The solid gray lines show the electric field of the laser pulse. The cyan arrows indicate the recollisions.

In order to obtain a clear physical interpretation of the mechanism properties of the multiple-recollision process, in Fig. 3 we show the correlative time distributions at three different intensities of 0.6, 0.8, and 1.2×10^{14} W/cm^2 from the top to the bottom, respectively. We use different abbreviated subscripts of time "t" for simplicity that "r" for recollision

time, "SI" for the first ionization time of the recollision electron, and "DI" for double ionization time. For the traveling time distribution of the NSDI trajectories where there is only one recollision for the three intensities [Figs. 3(a), 3(d) and 3(g)], the more prominent peaks located at nearly $0.6T$, $1.7T$, and $2.7T$, corresponding to the odd order of returning and the smaller peaks located at $1.2T$ and $2.2T$, corresponding to the even order of returning. As is known, the maximum returning energy of the odd order is always greater than the maximum returning energy of the even order, and the energy of the second returning electron is certainly smaller than $3.17U_p$ (U_p is the ponderomotive energy).[50] Thus, for the even order of returns the energy transferred from the recollosion electrons is not competent to ionize or even excite the bound electrons. So the peaks for the multiple-return trajectories are depressed in Figs. 3(a), 3(d), and 3(g). In Figs. 3(b), 3(e) and 3(h), for double-recollision events, the traveling time for the first recollision (black triangles) is about $0.6T$. Namely, the first collision occurs mainly at the first returning. Relatively, the traveling time distribution of the second recollisions (green squares) is uniform. At the intensity of 0.6×10^{14} W/cm^2 [Fig. 3(b)], the second collision occurs mainly at the second returning. But with the increasing of the intensity, the contribution of the later returns grow. This indicates that at the high intensity of 1.2×10^{14} W/cm^2 [Fig. 3(h)] the velocity of the recollision electron at the second return is fast enough so that interaction between the two electron is weak and the energy exchanged by recollision electron is not enough to directly ionize the struck electron. That results in the failed recollision events and the recollision electron needs a third or more return to transfer enough energy. Figures 3(c), 3(f) and 3(i) present the time delay between the double ionization and the last recollision for the single-recollision and double-recollision NSDI events, respectively. We can see the main peak of time delay distribution for double-recollision events (blue triangles) located at $0.25T$ for the three intensities, which means the two electrons get ionized as soon as the laser electric field reaches the peak. But for single-recollision trajectories, the time delay distribution for different intensities appears diverse. At the intensity of 0.6×10^{14} W/cm^2 [Fig. 3(c)], the main peak is shifted about $0.55T$, which is close to the second peak value of the time delay distribution of double-recollision events. For intensity of

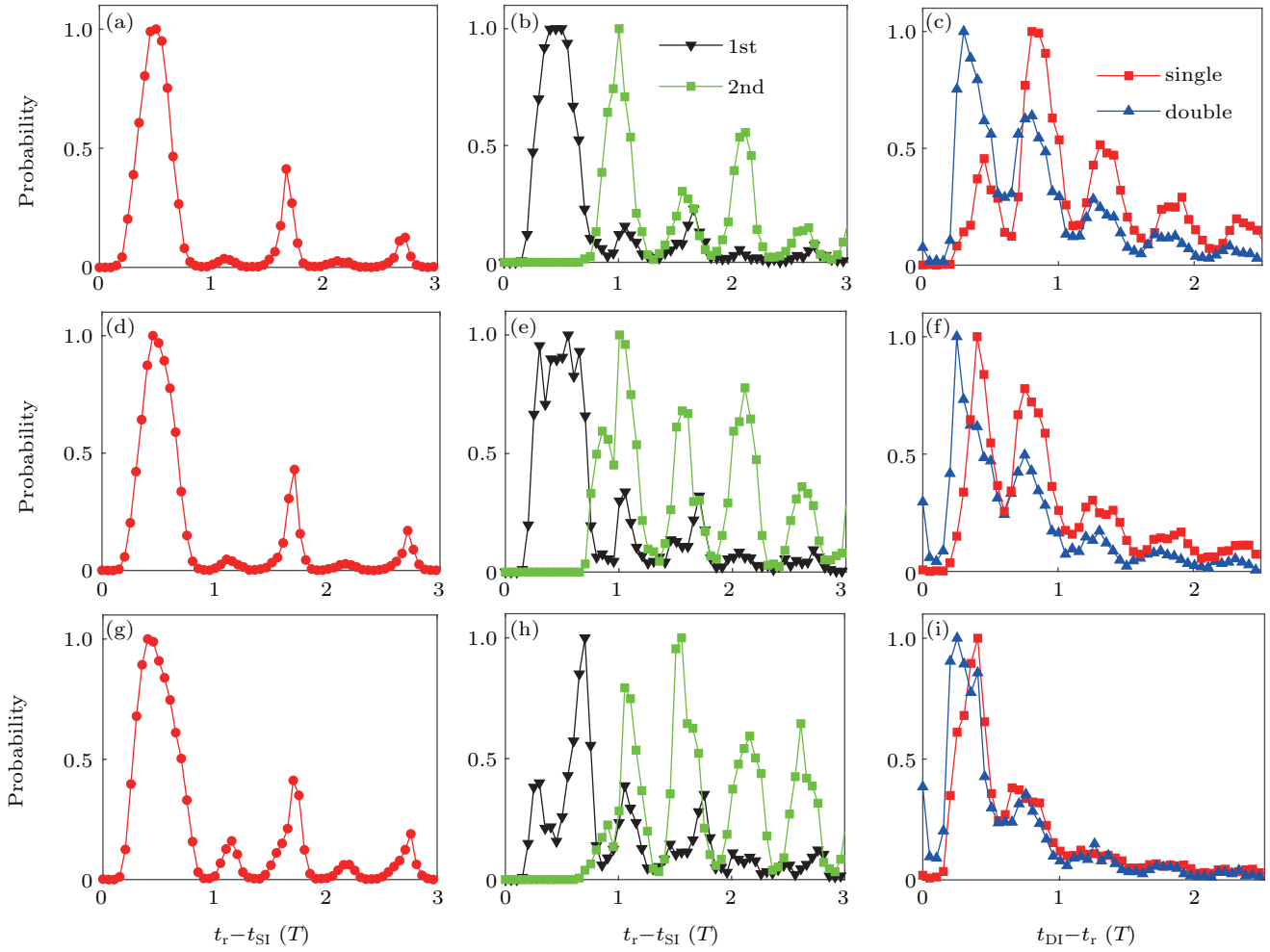


Fig. 3. The panels from top to bottom show the related time distribution at intensity of 0.6, 0.8, and 1.2×10^{14} W/cm^2, respectively. Left column: Traveling time for the NSDI trajectories where there is only one recollision. Middle column: Time difference between the first recollision and tunneling ionization (black triangles), the second recollision and tunneling ionization (green squares) for the double-recollision NSDI events. Right column: Time delay between the double ionization and the last recollision for the single-recollision (red squares) and double-recollision (blue triangles) NSDI events, respectively.

0.8×10^{14} W/cm^2 [Fig. 3(f)], the time delay focuses on $0.4T$. As the intensity increases to 1.2×10^{14} W/cm^2, as is shown in Fig. 3(i), the main peak almost overlaps with the time delay distribution of double-recollision events. The discussed above indicates that the ionization speed of the double-recollision trajectories is higher than that of the single-recollision trajectories. That is not difficult to understand, because the total energy transferred through the twice recollision is higher than that through one recollision. As a result, at low intensity the system is staying at a higher excited state after twice recollisions and the struck electron can escape more easily and fast. However, when the laser intensity increases, the returning energy of the electron is enhanced enough to pay for the excitation energy or ionization energy. Thus no matter there is one or two recollisions, the struck electron could be excited or ionized quickly.

In the following, to describe the energy exchange in the multiple recollision process detailedly, we perform the time evolution of the energies of electron pair belonging to the single-recollision and double-recollision trajectories in Figs. 4 and 5, respectively. For simplicity but without loss of generality, we choose the case of 0.8×10^{14} W/cm^2. In Fig. 4, plot (a) corresponds to the time $t = 1.7T$ when the recollision electrons begin to single ionization and plot (b) corresponds to the time $t = 2.0T$ that almost all recollision electrons have been ionized out of the nuclear. According to the recollision picture, the recollision electron returns every half cycle until the DI occurs. At time $t = 2.5T$, the DI trajectories resulted from the first return are clearly presented by the part in which both energies of the two electrons are more than zero. Because most of the time delay for single-collision events is longer than $0.5T$ [Fig. 3(f)], so we can see in plot (c) a part of energy distribution of the recollision electron (red circle lines) and the struck electron (blue diamond lines) is less than zero and more than -0.5, i.e., the doubly excited state, leaving the rest of bound electron which has not undergone impact is still in the bound state. In the classical model, the doubly excited states describe such a picture that the first electron excited the bound electron through the recollision but the recollision electron itself is recaptured, as shown by the classical trajectories in the first row of Fig. 2. Then every about $0.5T$, the recollision electrons return to excite or ionize the bound electrons until double ionization. We can see the number of bound electrons decreases gradually. Finally, all the electrons get released [plot (i)].

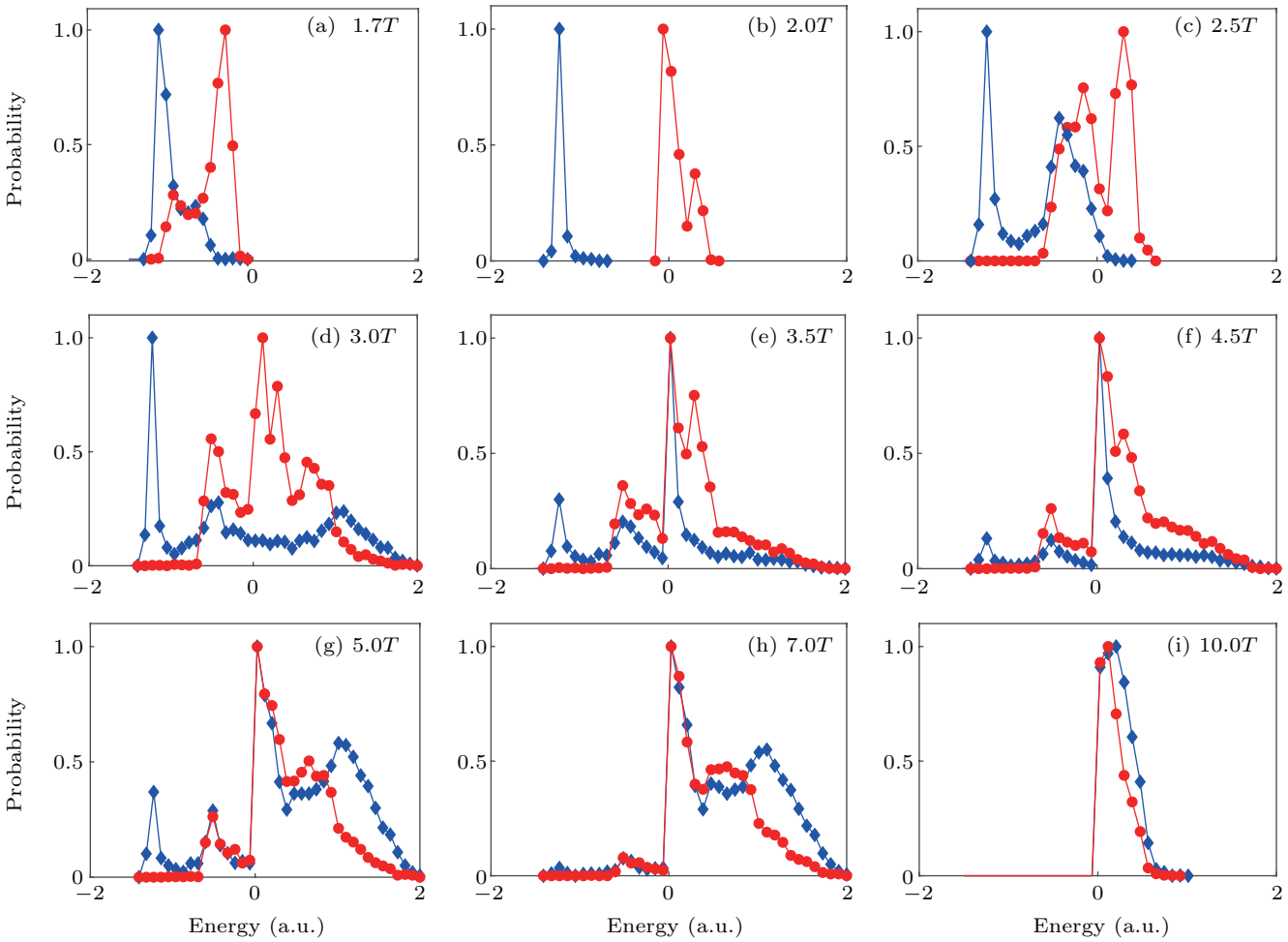


Fig. 4. Snapshots of the energy distribution as time evolves from $1.7T$ to $10.0T$ of NSDI trajectories selected from single-recollision events. The intensity is 0.8×10^{14} W/cm^2. In order to observe more clearly, we only show the trajectories single ionized at about $1.75T$ of the sine-shaped field. The red and blue lines indicate the recollision electrons and struck electrons, respectively.

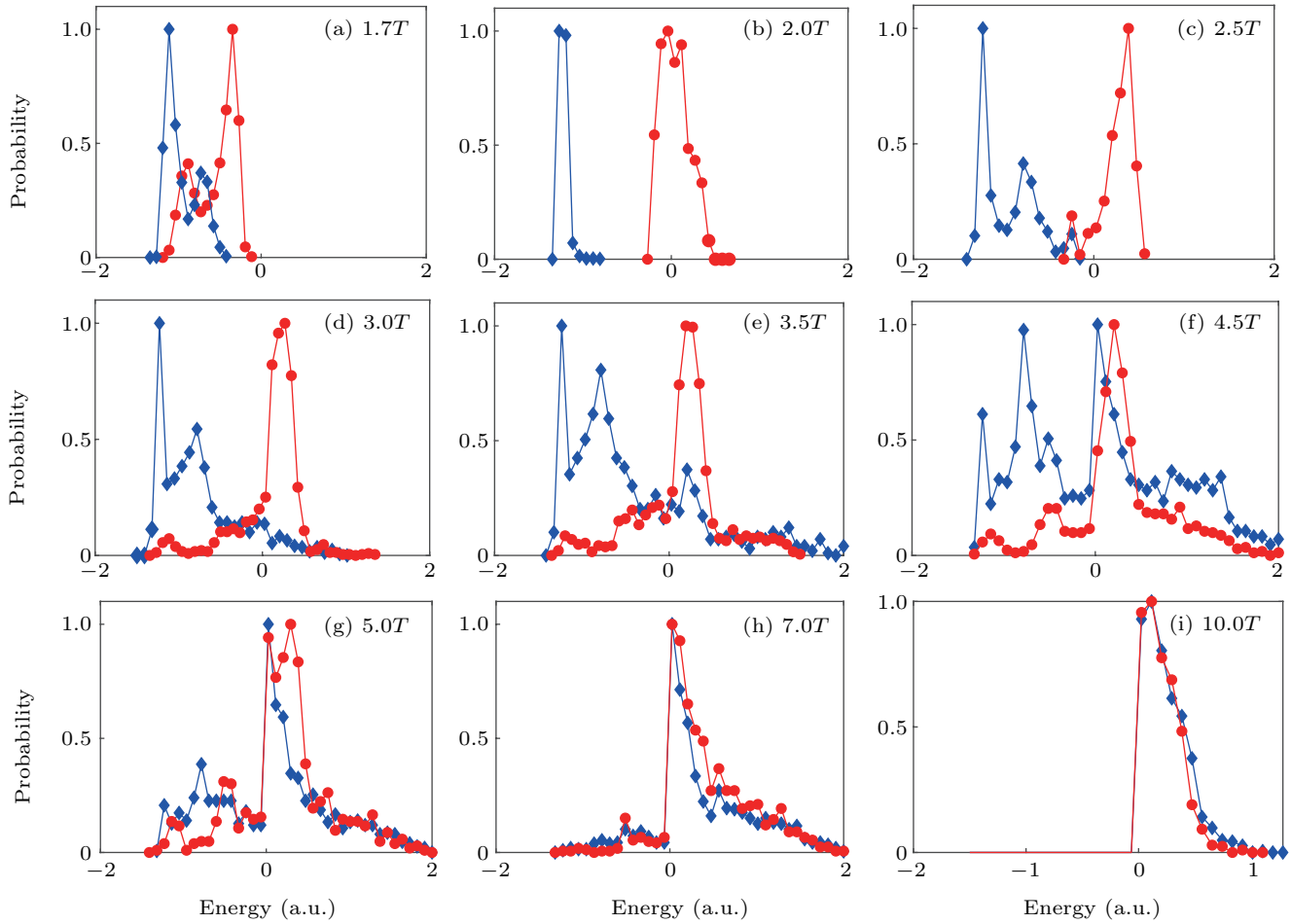


Fig. 5. Same to Fig. 4 but for NSDI trajectories selected from double-recollision events.

Comparatively speaking, the time evolution of double-recollision trajectories in Fig. 5 seems more complex. Even at time $t = 2.5T$, after the first recollision, most of the struck electrons stay in the bound or excited state and scarcely any get ionized. Figure 3(e) shows the time difference between the second recollision, and the tunneling ionization is more than $0.8T$. These struck electrons are still in excited state waiting for the second recollision from the recollision electrons' another returning. After another period of traveling time of nearly $0.6T$, some pairs of electrons stayed in doubly excited state undergo the second recollision and begin to get ionized at time $t = 3.5T$. Figure 5(f) shows at time $t = 4.5T$ the remaining bound electrons experience the second recollision at the recollision electrons' third or fourth returns. Through the multiple-recollision process the recollision electrons exchange more energy to the bound ones, increasing the final energy of struck electron and forming the significantly broaden sum-energy spectrum in Fig. 5(i).[35]

4. Conclusion

In summary, we revisited the recollision mechanism of NSDI below the recollision-ionization threshold using a linearly polarized driving laser field of 780 nm and found the contribution of multiple recollisions is prevalent at lower intensities. Compared with the single-recollision process, the multiple-recollision promotes the energy exchange from the recollision electron to the bound electron. Thus for multiple-recollision events, the energies of doubly excited states are higher and the DI occurs more quickly than single-recollision trajectories. We also studied the time evolution of energy by tracing trajectories, which provides illustration about the process of multiple recollisions.

References

[1] I'Huillier A, Lompre L A, Mainfray G and Maus C 1983 *Phys. Rev. A* **27** 2503
[2] Fittinghoff D N, Bolton P R, Chang B and Kulander K C 1992 *Phys. Rev. Lett.* **69** 2642
[3] Walker B, Sheehy B, DiMauro L F, Agostini P, Schafer K J and Kulander K C 1994 *Phys. Rev. Lett.* **73** 1227
[4] Larochelle S, Talebpoury A and Chin S L 1998 *J. Phys. B* **31** 1201
[5] Becker A and Faisal F H M 2000 *Phys. Rev. Lett.* **84** 3546
[6] Kopold R, Becker W, Rottke H and Sandner W 2000 *Phys. Rev. Lett.* **85** 3781
[7] Schafer K J, Yang B, DiMauro L F and Kulander K C 1993 *Phys. Rev. Lett.* **70** 1599
[8] Corkum P B 1993 *Phys. Rev. Lett.* **71** 1994
[9] Feuerstein B, Moshammer R, Fischer D, Dorn A, Schröter C D, Deipenwisch J, Crespo López-Urrutia J R, Höhr C, Neumayer P, Ullrich J, Rottke H, Trump C, Wittmann M, Korn G and Sandner W 2001 *Phys. Rev. Lett.* **87** 043003

[10] Wang F, Liu K, Zhang X F, Wang Z, Qin M Y, Liao Q and Lu P X 2019 *Phys. Rev. A* **100** 043405
[11] Wang F, Liao Q, Liu K, Qin M Y, Zhang X F, Zhang Q B, Cao W, Pi L W, Zhou Y M and Lu P X 2021 *Phys. Rev. A* **103** 013115
[12] Liao Q, Li Y, Qin M Y and Lu P X 2017 *Phys. Rev. A* **96** 063408
[13] Weber T, Giessen H, Weckenbrock M, Urbasch G, Staudte A, Spielberger L, Jagutzki O, Mergel V, Vollmer M and Dörner R 2000 *Nature* **405** 658
[14] Moshammer R, Ullrich J, Feuerstein B, Fischer D, Dorn A, Schröter C D, Crespo López-Urrutia J R, Höhr C, Rottke H, Trump C, Wittmann M, Korn G, Hoffmann K and Sandner W P 2003 *J. Phys. B* **36** L113
[15] Eremina E, Liu X, Rottke H, Sandner W, Dreischuh A, Lindner F, Grasbon F, Paulus G G, Walther H, Moshammer R, Feuerstein B and Ullrich J 2003 *J. Phys. B* **36** 3269
[16] Weckenbrock M, Becker A, Staudte A, Kammer S, Smolarski M, Bhardwaj V R, Rayner D M, Villeneuve D M, Corkum P B and Dörner R 2003 *Phys. Rev. Lett.* **91** 123004
[17] Weckenbrock M, Zeidler D, Staudte A, Weber Th, Schöffler M, Meckel M, Kammer S, Smolarski M, Jagutzki O, Bhardwaj V R, Rayner D M, Villeneuve D M, Corkum P B and Dörner R 2004 *Phys. Rev. Lett.* **92** 213002
[18] Zeidler D, Staudte A, Bardon A B, Villeneuve D M, Dörner R and Corkum P B 2005 *Phys. Rev. Lett.* **95** 203003
[19] Liu Y Q, Fu L B, Ye D F, Liu J, Li M, Wu Ch Y, Gong Q H, Moshammer R and Ullrich J 2014 *Phys. Rev. Lett.* **112** 013003
[20] Liu X and Figueira de Morisson Faria C 2004 *Phys. Rev. Lett.* **92** 133006
[21] Huang C, Zhou Y M, Zhang Q B and Lu P X 2013 *Optics Exp.* **21** 11382
[22] Tong A H, Zhou Y M and Lu P X 2015 *Optics Exp.* **23** 15774
[23] He L X, Lan P F, Zhang Q B, Zhai C Y, Wang F, Shi W J and Lu P X 2015 *Phys. Rev. A* **92** 043403
[24] Li Y, Lan P F, Xie H, He M R, Zhu X S, Zhang Q B and Lu P X 2015 *Optics Exp.* **23** 28801
[25] Li M, Zhang P, Luo S Q, Zhou Y M, Zhang Q B, Lan P F and Lu P X 2015 *Phys. Rev. A* **92** 063404
[26] Staudte A, Ruiz C, Schöffler M, Schössler S, Zeidler D, Weber T, Meckel M, Villeneuve D M, Corkum P B, Becker A and R Dörner 2007 *Phys. Rev. Lett.* **99** 263002
[27] Chen Zh J, Liang Y Q and Lin C D 2010 *Phys. Rev. Lett.* **104** 253201
[28] Rudenko A, de Jesus V L B, Ergler Th, Zrost K, Feuerstein B, Schröter C D, Moshammer R and Ullrich J 2010 *Phys. Rev. Lett.* **99** 263003
[29] Zhou Y M, Liao Q and Lu P X 2010 *Phys. Rev. A* **82** 053402
[30] Camus N, Fischer B, Kremer M, Sharma V, Rudenko A, Bergues B, Kübel M, Johnson N G, Kling M F, Pfeifer T, Ullrich J and Moshammer R 2012 *Phys. Rev. Lett.* **108** 073003
[31] Blaga C I, Catoire F, Colosimo P, Paulus G G, Muller H G, Agostini P and DiMauro L F 2009 *Nat. Phys.* **5** 335
[32] Quan W, Lin Z, Wu M, Kang H, Liu H, Liu X, Chen J, Liu J, He X T, Chen S G, Xiong H, Guo L, Xu H, Fu Y, Cheng Y and Xu Z Z 2009 *Phys. Rev. Lett.* **103** 093001
[33] Wu C Y, Yang Y D, Liu Y Q, Gong Q H, Wu M, Liu X, Hao X L, Li W D, He X T and Chen J 2012 *Phys. Rev. Lett.* **109** 043001
[34] Pullen M G, Dura J, Wolter B, Baudisch M, Hemmer M, Camus N, Senftleben A, Schroeter C D, Moshammer R, Ullrich J and Biegert J 2014 *J. Phys. B* **47** 204010
[35] Liu Y Q, Tschuch S, Rudenko A, Dürr M, Siegel M, Morgner U, Moshammer R and Ullrich J 2008 *Phys. Rev. Lett.* **101** 053001
[36] Ye D F, Li M, Fu L B, Liu J, Gong Q H, Liu Y Q and Ullrich J 2015 *Phys. Rev. Lett.* **115** 123001
[37] Wolter B, Pullen M G, Baudisch M, Sclafani M, Hemmer M, Senftleben A, Schröter C D, Ullrich J, Moshammer R and Biegert J 2015 *Phys. Rev. X* **5** 021034
[38] Panfili R, Haan S L and Eberly J H 2002 *Phys. Rev. Lett.* **89** 113001
[39] Ho Phay J, Panfili R, Haan S L and Eberly J H 2005 *Phys. Rev. Lett.* **94** 093002
[40] Haan S L, Van Dyke J S and Smith Z S 2008 *Phys. Rev. Lett* **101** 113001
[41] Ye D F, Liu X and Liu J 2008 *Phys. Rev. Lett.* **101** 233003
[42] Zhou Y M, Liao Q and Lu P X 2009 *Phys. Rev. A* **80** 023412
[43] Zhou Y M, Huang C, Liao Q and Lu P X 2012 *Phys. Rev. Lett* **109** 053004
[44] Zhou Y M, Zhang Q, Huang C and Lu P X 2012 *Phys. Rev. A* **86** 043427
[45] Xu T T, Ben S, Wang T, Zhang J, Guo J and Liu X S 2015 *Phys. Rev. A* **92** 033405
[46] Tong A H, Li Q G, Ma X M, Zhou Y M and Lu P X 2019 *Optics Exp.* **27** 6415
[47] Huang C, Zhong M and Wu Z 2018 *Sci. Rep.* **8** 8772
[48] Ma X M, Zhou Y M, Li N, Li M and Lu P X 2018 *Optics and Laser Technology* **108** 235
[49] Ma X M, Zhou Y M, Chen Y B, Li M, Li Y, Zhang Q B and Lu P X 2019 *Optics Exp.* **27** 1825
[50] Becker W, Grasbon F, Kopold R, Milosevic D B, Paulus G G and Walther H 2002 *Adv. At. Mol. Opt. Phys.* **48** 35